J Solid State Electrochem (1999) 3: 87–96

ORIGINAL PAPER

Mikołaj Donten

Bulk and surface composition, amorphous structure, and thermocrystallization of electrodeposited alloys of tungsten with iron, nickel, and cobalt

Received: 19 January 1998 / Accepted: 17 July 1998

Abstract It has been shown for iron-group alloys of tungsten, using ESCA spectroscopy of samples sputtered with argon ions and SEM/EDS analysis, that no oxygen is present in the alloy bulk. A very weak internal organization in the alloys, which follows from low and wide diffractograms usually obtained for electrodeposited layers, is thought to be a heavily distorted structure of the major metal component of the alloy. Thermal crystallization of thin layers of the amorphous tungsten alloys does not lead to formation of well-known intermetallic crystal structures.

Key words Tungsten alloys · Amorphous structure · Electron spectroscopy for chemical analysis · Bulk composition · Electrodeposition

Introduction

Amorphous metallic alloys became attractive in physics, engineering, and chemistry in the 1960 s, when rapid quenching became available as a relatively simple method of production of these alloys [1]. At the same time, electrochemical methods were developed which allowed production of amorphous metal films on various substrates [2, 3]. The more technologically advanced but less frequently used methods are those such as ion implantation [4], sputtering with beams of inert-gas ions [4], mechanical alloying [5], and transformation of crystals into amorphous materials under ultrahigh pressure [6].

Electrodeposition of tungsten alloys on various substrates is of practical significance because of their corrosion and wear resistance [7–10]. However, their potential ability to protect a particular substrate is often decreased by either poor adhesion to the substrate surface, or easy exfoliation, or cracking as a result of the existence of high internal stress. Electrodeposition of tungsten-containing alloys is an interesting electrochemical phenomenon, because tungsten cannot be plated alone from aqueous solutions [11].

In the literature, there are few data concerning the structure and composition of the amorphous tungsten alloys. The structure of the tungsten alloys obtained by electrodeposition is not perfectly amorphous. The X-ray diffractograms possess broad signals of low intensity [12, 13], which indicates that only a very limited assembling exists in the structure of these materials. An open question is whether the amorphous tungsten alloys contain significant amounts of oxygen. The aim of this paper is to address these problems by X-ray diffraction, scanning electron microscopy (SEM), energy dispersive X-ray spectroscopy (EDS), wave dispersive X-ray spectroscopy (WDS), and electron spectroscopy for chemical analysis (ESCA) studies of the tungsten alloys with cobalt, nickel, and iron.

Experimental

The depositions were performed with an EG&G PARC potentiostat/galvanostat model 173, which was controlled by a computer equipped with a National Instruments Lab PC 12-bit 48-channel ADDA card. The software, which allowed programming of a current waveform of arbitrary shape, was developed in our laboratory. Co-, Ni-, and Fe-W alloy layers were deposited on copper and platinum foils. Before experiments the foil was polished, washed with a detergent, and rinsed with water and acetone. This was followed by immersing the foil into a 5% H_2SO_4 solution for 20 s to activate the foil surface. The copper cathode (4 cm^2) was placed between two platinum anodes of areas 8 cm^2. Mass and thickness of the layers were determined by weighing. The composition of the plating bath was as given in the patent [12]: sodium tungstate (81.5 g/l), ammonia citrate (59 g/l), conc. (85%) phosphoric acid (7.69 ml/l), boric acid (10.25 g/l), 2-butene-2,4-diol (0.05 g/l), 25% ammonia solution to adjust the pH to 8.5, and $Co(NO_3)_2.x6H_2O$ (3.89 g/l), $NiSO_4$

M. Donten
Department of Chemistry,
University of Warsaw,
Pasreura 1,
PL-02-093 Warsaw, Poland
e-mail: donten@chem.uw.edu.pl, Fax: +48-22-8225996

(2.8 g/l), or $FeSO_4$ (2.8 g/l). BPO_4, which according to the patent procedure should be present at a concentration of 17.5 g/l, was replaced by H_3PO_4 (85%) and H_3BO_3 at concentrations of 7.69 ml/l and 10.25 g/l, respectively, which were added to the galvanic bath [13]. Separation of anodic and cathodic compartments by a glass frit avoided degradation of the plating bath solution [14].

The structure of the alloys deposited was determined by X-ray diffraction using a DRON-1 instrument with a cobalt X-ray lamp equipped with a CoKL filter. Optical inspection of the alloy surface was done with an inverted metallurgical microscope (Olympus, type PM3). Detailed observation of surface topography of the alloys and determination of composition of the alloys were done using a Leo Zeiss SEM model 435 VP, in conjunction with an X-ray EDS analyzer from Roentec (Germany), model M1. The instrument used for WDS analysis was from CAMECA (France), model SX-50. Surface composition analyses were done using ESCA spectroscopy equipped with an aluminum cathode.

The plating temperature was maintained at 65 °C. The current density of the deposition process was set at 35 mA/cm^2 for the Co and Fe alloys, and 70 mA/cm^2 for the Ni alloy. The volume and pH of the bath were corrected by adding water and ammonia, respectively. All solutions were prepared from analytical grade chemicals and deionized water.

Results

Electrodeposition of tungsten from aqueous solution is impossible. However, codeposition with one of the iron-group metals does occur. The mechanism of the process of electrodeposition of tungsten alloys is not well understood. It is believed that the codeposition consists of both electrochemical and chemical steps. The chemical steps, such as the reduction of tungsten compounds by elemental hydrogen formed at negative potentials, must accompany electrochemical processes and can depend on the plating potential and the pH of the plating solution. It usually makes the deposition process sensitive to the pH of the bath solution. The strong dependence of the rate of deposition on pH is shown in Fig. 1. It is surprising that the composition of the alloys deposited is practically constant for each type of alloy and, in the examined range, is almost independent of pH. The complexity of the mechanism of formation of amorphous deposits suggests that the alloys may contain more elements than just tungsten and an iron-group metal. It was proved by inductively coupled plasma analysis of a Co-W layer that small amounts of boron and phosphorus are present in the deposit. In four analyzed samples, boron was found at the level of 0.7–1.3 at% and phosphorus in three of them at about 1 at%. Experiments performed several years ago indicated that the deposition rate and quality of the alloy layers strongly depended on the presence of boron and phosphorus compounds in the plating bath solution [13]. Despite the fact that the amounts of phosphorus and boron in the alloys are always small and do not exceed 1.5 at%, their presence significantly improves the quality and mechanical properties of the alloys [12, 15].

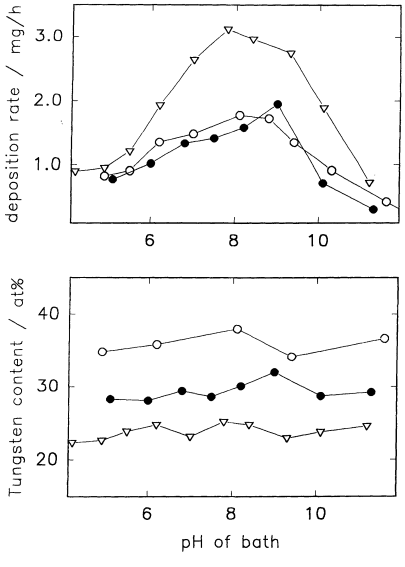

Fig. 1 Deposition rate and composition of Ni-W and Co-W alloys vs pH

Oxygen content in the deposits

A significant problem is oxygen contained in electrodeposited tungsten alloys. This fragmentary discussed issue is still unresolved. Rauscher et al. [16] examined Ni-W layers which were first detached from stainless steel substrates and then dissolved in boiling concentrated hydrochloric acid. They found tungsten oxides in the precipitate after dissolution of the samples. However, the materials examined by Rauscher et al. were deposited under different conditions to those described in the experimental section of this paper. To clarify the problem of oxygen content in the deposited layers we have carried out a series of WDS and ESCA analyses. No significant amounts of oxygen in the Co-W and Ni-W deposits were found by the WDS analysis. In these experiments, oxygen was detected at a level of 1–3 at%. The source of this small amount of oxygen was probably the surface layer of the material, which is usually oxidized by atmospheric oxygen. A more detailed and reliable study was done by carrying out a series of ESCA measurements with samples of Co-W and Ni-W deposits. The results of the Co-W sample analysis were obtained for the alloy composition $W_{29}Co_{71}$. Before sputtering, the surface contained, in addition to W and Co, also O, C, and even some amounts of Na and Si. The ESCA spectrum and the result of the qualitative composition analysis are shown in Fig. 2. The presence of carbon and silicon is due to contamination by hydrocarbons/dust adsorbed from the atmosphere during storage of the samples in air. It can be concluded from the spectra that W and Co exist in both oxidized and unoxidized forms in the surface region. For example, the tungsten W 4*f* spectrum (Fig. 3A) consists of peaks for both metallic and oxygen-bonded tungsten. The signals of metallic tungsten can be found at about 31.5 eV and 33.5 eV. It is not possible to find out whether these signals correspond to a pure phase of tungsten or to

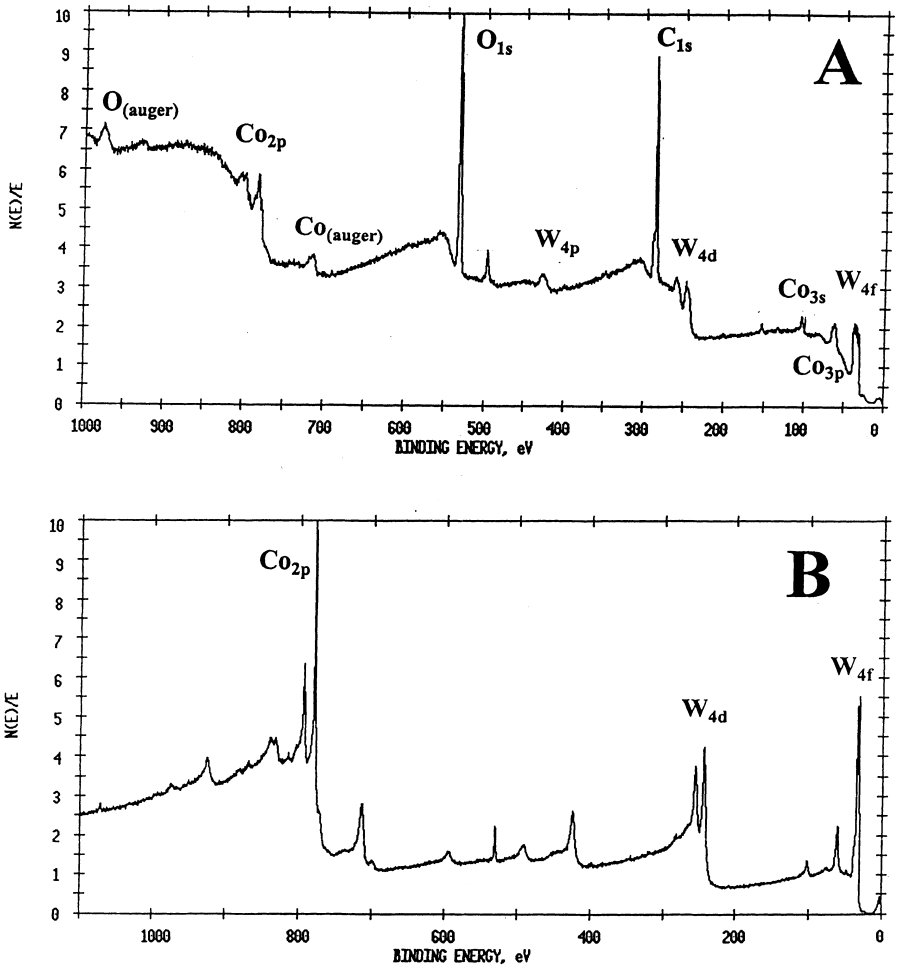

Fig. 2A, B Electron spectroscopy for chemical analysis (ESCA) spectra of analyzed Co-W alloy. **A** sample before sputtering; **B** after 195 s of sputtering

tungsten in the tungsten-cobalt alloy. The oxide peaks are placed at 36 eV and 38 eV, and these energies are close to those expected for WO_3. The Co spectrum (Fig. 4A) also contains peaks corresponding to metallic Co and CoO. These effects may occur when the surface is covered with a thin oxide film. The thickness of the oxide film has been estimated as approximately 50–60 Å. A quantitative analysis of the results obtained for the non sputtered sample gave a mean concentration of oxygen in the surface layer of 61 at%.

Sputtering of the samples with argon for 75 s removes most of the oxygen. A prolonged sputtering, up to 195 s, leads to a further decrease of the oxygen content in the analyzed layer. The spectra presented in Fig. 2B, 3B, and 4B indicate that the surface of the alloy is oxygen-free. The depth of a 195-s sputtering cannot be exactly determined; it can be estimated as 150–300 Å. The oxygen traces seen in the spectra after sputtering may be due to the effect of remaining oxide in the so-called "sputter shadow". This is a geometrical effect observed on rough surfaces. Taking this effect into account, the 2 at% of oxygen found on the surface of the 195-s sputtered sample can be neglected.

The results obtained for the Ni-W alloy samples were similar to those for the Co-W alloy. About 1–5 at% of oxygen were found in a sample of this alloy in WDS analyses. The amount of oxygen detected in long-stored (6 weeks or longer) samples was higher, which suggests that the surface was the source of the oxygen signal detected in the WDS spectra. An analysis of the surface composition of the Ni-W alloy made by ESCA supported the suspicion about the presence of oxygen only in a thin external layer of the alloy. Before sputtering the surface was covered by tungsten and nickel oxides; therefore an intensive oxygen O 1*s* signal was obtained for the nonsputtered sample surface. This signal was not seen for the long-time (at least 3 min) sputtered samples. The changes which were observed in the nickel and tungsten electron spectra proved that on the surface of the alloy both elements exist in the oxide form. In the case of the Ni-W alloy ($Ni_{79}W_{21}$), the content of oxygen in the surface layer, determined for the nonsputtered sample, was 57 at%. A slightly lower content of oxygen in the $Ni_{79}W_{21}$ alloy compared to $Co_{71}W_{29}$ can be explained by a decrease of the amount of tungsten trioxide. Also, in the case of Ni-W amorphous alloy, an estimated thickness of the surface layer containing oxygen is in the range of 200 Å. It means that the bulk material contains no oxygen. The spectra shown in Fig. 5 and 6 indicate that there are some changes in the oxidation state of

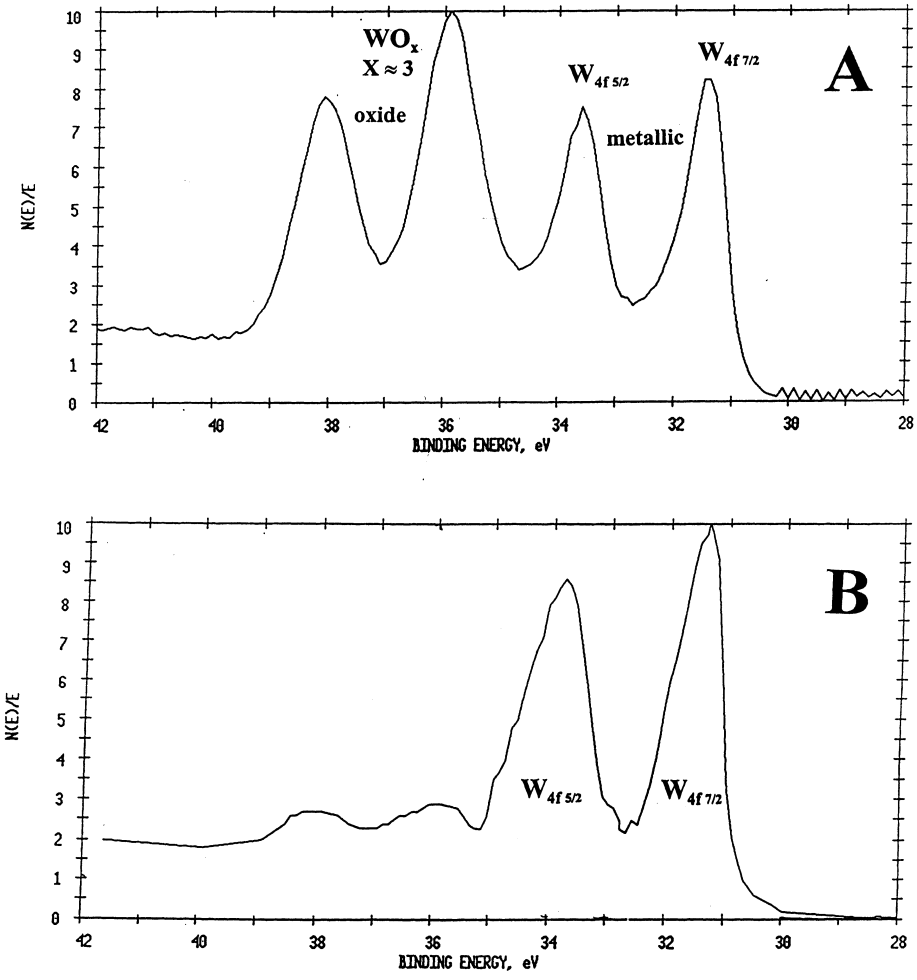

Fig. 3A, B ESCA spectra of tungsten 4*f* electrons (W 4*f*) before (**A**) and after 195 s of sputtering (**B**)

tungsten (W 4*d* electrons) and nickel (Ni 2*p* electrons) present in the surface and the inner layers of the alloy coverage. These changes affect the shape and peak position of the W 4*d* and Ni 2*p* electrons. The spectra in Fig. 5A and 6A are typical for a mixture of WO_3 and W, and NiO and Ni, respectively. From the shape and relative intensity of the signals of oxidized and unoxidized metals, the thickness of the surface oxides can be estimated as 50–70 Å. Another argument that is in favor of a small thickness of the oxide layer is the fact that it is completely removed during 300 s of sputtering. The spectra shown in Fig. 5B and 6B were recorded after sputtering and contain W 4*d* and Ni 2*p* peaks typical for pure, unoxidized metals. The ESCA results obtained for the Ni-W amorphous alloy fit well to the WDS results obtained for this alloy.

Good agreement between the results obtained for the Ni-W and Co-W alloys allows us to expect that the Fe-W alloy, which is electrodeposited under similar conditions, has no oxygen in the bulk.

A series of micrographs obtained by SEM and supported by an on-line EDS analysis helped to judge finally the presence of oxides in the amorphous deposits. Since it is possible that oxides can be present in the alloys deposited under the conditions different from those given in the experimental section of this work, Fe-W alloy layers were deposited under optimum and off-optimum conditions. Figure 7 shows two representative micrographs. A rough surface with crystals on it, shown in Fig. 7B, was obtained from deposition in a bath at pH 5.5, which is a relatively low value for this process. The current density was lower by half, which helped to avoid the effect of a decreasing concentration of hydrogen ions in the area next to the cathode surface. EDS analysis performed at the spots containing a large number of crystalline plates, as seen at the lower right corner of Fig. 7B, indicated that the oxygen content is above 50 at%. The same analysis of the surface fraction without the plates, such as that shown in the middle of the picture, indicated that the content of oxygen is very low. The amount of oxygen detected in this place is within the accuracy of the EDS method. Not surprisingly, for the alloy sample deposited under the optimal conditions (Fig. 7A), no oxides in the alloy were seen or detected. The incorporation of oxide plates in the deposits is most intensive in the case of the Fe-W alloy, but is also observed in the case of the Co-W and Ni-W alloys. An explanation of this phenomenon can be de-

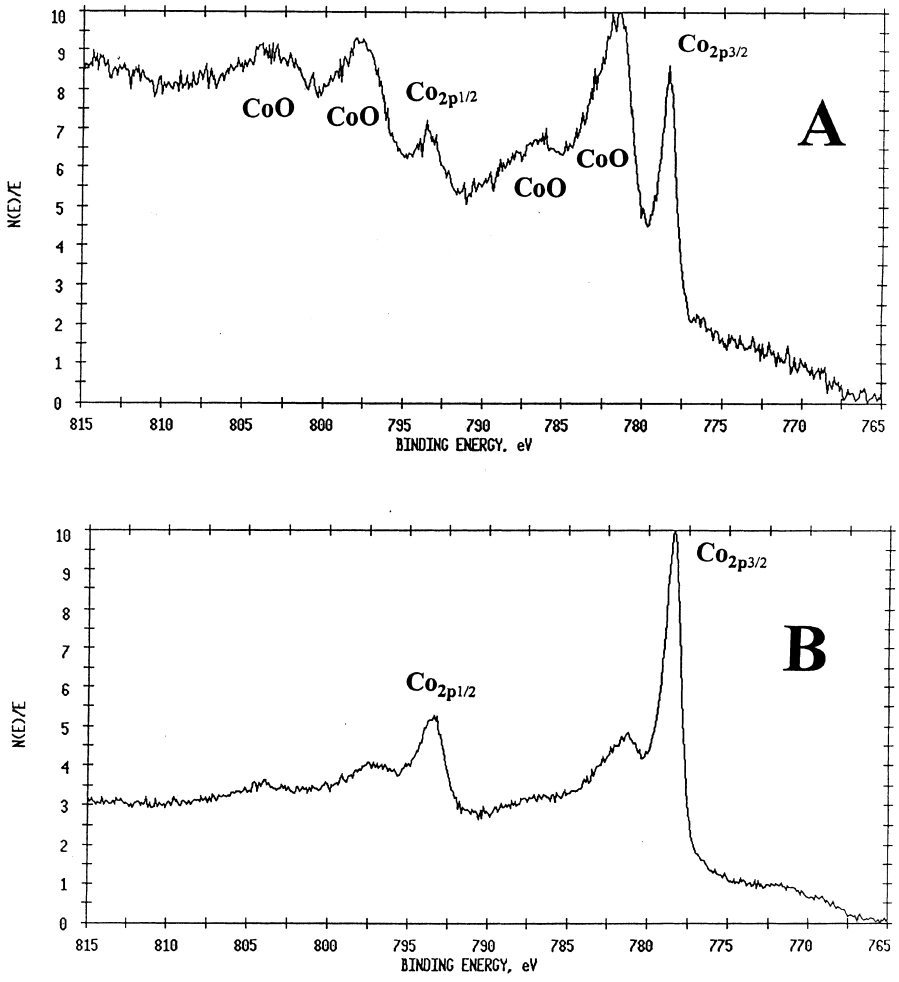

Fig. 4A, B ESCA spectra of cobalt 2*p* electrons (Co 2*p*) before (**A**) and after 195 s of sputtering (**B**)

duced from the comparison of the tungsten content in the deposited alloys (Fig. 1). The formation of oxide plates is more pronounced for the alloys with the highest content of tungsten, which supports the idea that the plates are built of tungsten oxides.

Composition of the alloys

The existence of peaks in the X-ray spectra of the tungsten amorphous alloys indicates that the alloys are not perfectly amorphous. The problem of some ordering within the amorphous alloys has been discussed in the literature [17–19]. It is rather improbable that the distances between the atoms and their orientation in the alloys are completely random. The constant composition of the deposited alloys is also in favor of the existence of quasi-structures typical for each alloy studied. Very probably, the X-ray diffractograms reflect the presence of some elements of the structure of the major component of the alloy, e.g. the Ni-W alloy may have elements of the nickel metallic structure, the Co-W alloy may acquire locally some structure from cobalt, and the Fe-W alloy from iron. To verify this hypothesis, an examination of the X-ray diffractograms of all three kinds of tungsten alloys was carried out. Figure 8 shows typical X-ray diffraction patterns. Two of them, which were obtained for the Co-W and Ni-W alloys, exhibit almost identical shapes. The third diffraction pattern slightly differs from the other two and was obtained for the Fe-W alloy. All three peaks obtained for the amorphous materials are located close to the most intense lines of crystalline nickel, cobalt, and iron, respectively. Table 1 presents the peak positions for crystalline, pure metals and their amorphous alloys with tungsten. An apparent increase in the lattice constants has been found. The increase in lattice constants, calculated from the location of the maximum of the diffraction peaks, is caused by an increase in the mean inter-atom distances, which is a result of implanting tungsten in the structures of nickel, cobalt, and iron. The influence of the tungsten content in the amorphous alloys on the mean lattice constant is shown in Table 2. There is a clear regularity: an increase in the tungsten content in all the alloys leads to an increase in mean interatom distances in the deposited layers. This kind of change in the crystalline structures is described by the Vegard rule, which says that the lattice parameter of a constituted alloy is a linear combination of the lattice parameters of the components. In the crystalline state, for all three alloys, there is a strictly

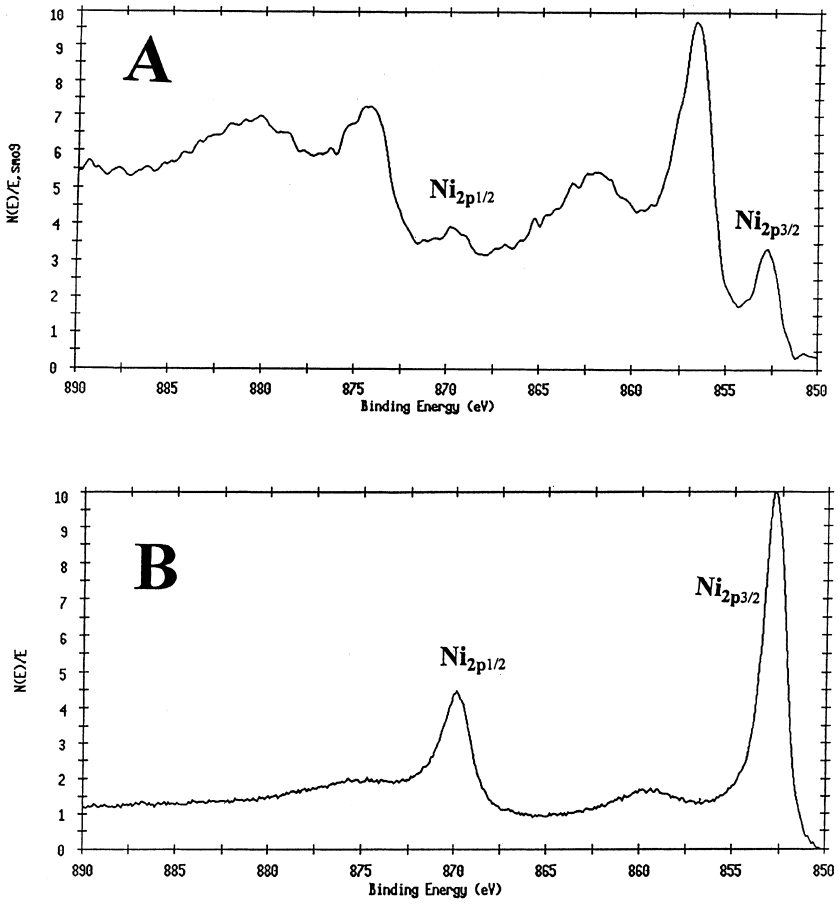

Fig. 5A, B ESCA spectra of tungsten 4*d* electrons (W 4*d*) before (**A**) and after 300 s of sputtering (**B**)

linear dependence of the lattice constant of the major component versus the content of tungsten in the alloy [20]. Such an effect is typical for alloys which have an internal structure of a solid solution based on the structure of the major component.

The X-ray diffraction data may be interpreted in the way that the tungsten alloys, obtained by electrodeposition, have severely deformed structures of the major component. However, there is a phenomenon that should be addressed here: for each kind of alloy the content of tungsten in the deposits is, in a wide range, independent of both pH and concentration of the iron-group metal in the bath. On the other hand, the amounts of tungsten in the deposits are different for the Co, Ni, and Fe based alloys. An analysis of the phase diagrams of the tungsten binary alloys [20–23] may suggest that the compositions of tungsten-containing amorphous alloys are close to those of the intermetallic compounds which are formed between tungsten and the codeposited metals. The most common and thermodynamically stable compounds of tungsten and iron-group metals are listed in Table 3. From the data shown it is clearly seen that the compositions of the electrodeposited alloys are determined by the compositions of the intermetallic compounds formed by iron-group metals and tungsten. These compounds are Ni_4W, Co_3W, and Fe_2W for nickel, cobalt, and iron alloys, respectively. For the constant current deposition applied in this work, in every case the alloy composition is close to the compound containing the lowest amount of tungsten.

Changes in the alloy structure caused by heating

In the hope of obtaining more information on the problems mentioned above, an X-ray diffraction analysis of the thermally crystallized alloys has been performed. This study was limited to the Ni-W alloy. Figures 9 and 10 present the diffraction patterns of the thermally crystallized alloy. The changes in the alloy surface morphology caused by the heating can be seen using an optical microscope. The surface of the annealed samples was dull and a delicate crystalline pattern appeared. The color of the alloy surface changed to gray and green, which is characteristic for a mixture of the oxides of tungsten and nickel. As can be seen in Fig. 9, the thermally induced changes in the internal structure of the alloy, detectable by X-ray diffraction spectroscopy, start at a temperature higher than 200 °C. Figure 10 shows the changes in the internal structure of the alloy subjected to heating at 400 °C. The patterns obtained for the layers heated for 1 and 4 h are essentially the same. The absence of new diffraction peaks proves that

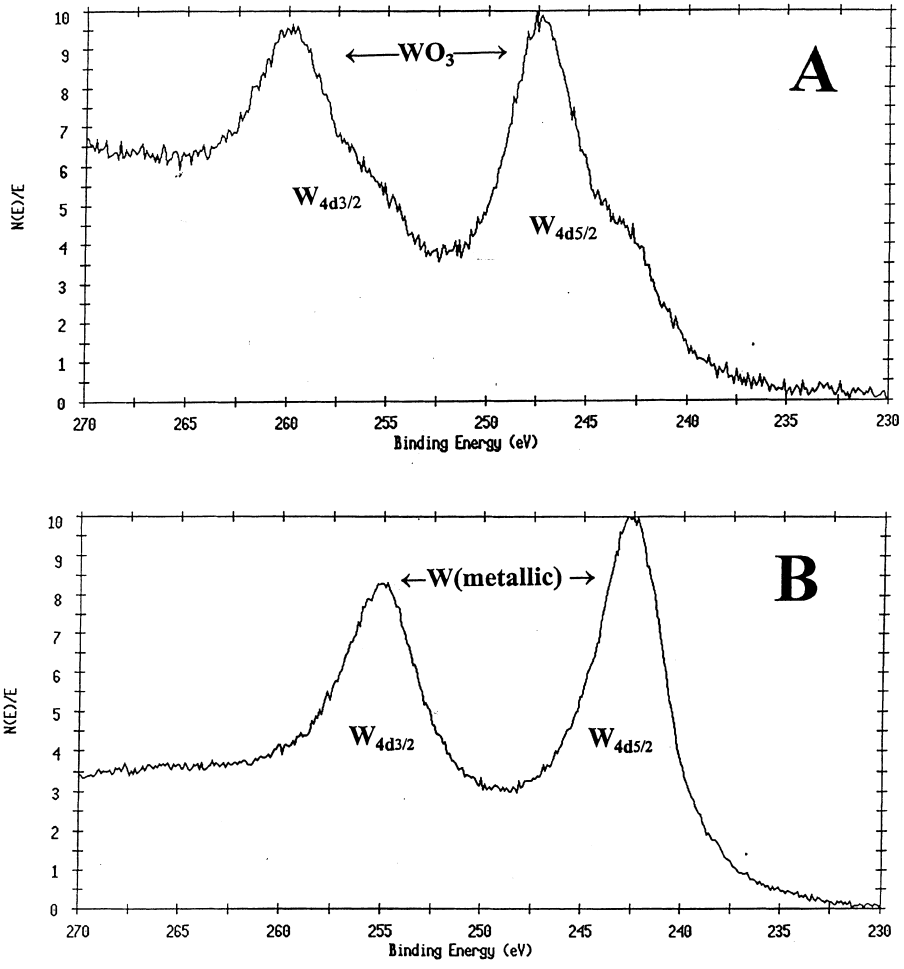

Fig. 6A, B ESCA spectra of nickel 2*p* electrons (Ni 2*p*) before (**A**) and after 300 s of sputtering (**B**)

the formation of new phases does not occur. It is possible that a structure similar to a solid solution of tungsten in nickel [20] is formed under these conditions. The structure of this material is identical to the cubic structure of pure nickel. The lattice constant increases proportionally to the tungsten content in the alloy.

An examination of the magnetic properties of the heated Ni-W samples confirms that the structural changes in the alloy start at temperature slightly above 200 °C. However, the process proceeds slowly. The magnetic analyses did not establish a well-defined temperature limit, which is characteristic for a phase transformation. Above 500 °C, the formation of new structures is observed, but the crystallization process is not completed after 2 h of heating at 650 °C. The group of signals seen on diffractogram E in Fig. 9 cannot be easily matched with the crystallographic structures known for tungsten, nickel, or their intermetallic compounds. It is probable that longer heating of the sample may lead to further transformation of the metastable forms obtained and converts the alloys to thermodynamically stable intermetallic compounds. It is known that a very long period of annealing is necessary for completing the transformation of alloys formed by tungsten and iron-group metals into crystalline intermetallic compounds. The ΔG of formation of those compounds is in the range of –1 to –5 kJ/mol [21–23]. The possibility of the formation of compounds between the substrate and the deposited layers may additionally complicate X-ray diffractograms. To avoid such a complication, either thick, over 20-mm, layers should be examined or the deposit should be separated from the substrate before heat treatment. This was not tried in the frame of this work.

Summary

The results described above disprove the presence of significant amounts of oxygen in the alloys. Oxygen was found in oxides in the surface layer only, and could be removed quantitatively by sputtering the surface with argon. The results obtained are not consistent with the results obtained by Rauscher's et al. [16]. However, the alloys examined in Rauscher's work were deposited from a bath solution containing nickel at a level 10 times higher than that of this work. This resulted in a slower deposition of the material. The small deposition rate and the intensive hydrogen evolution create conditions which help to avoid inclusion of oxides in the metallic layers.

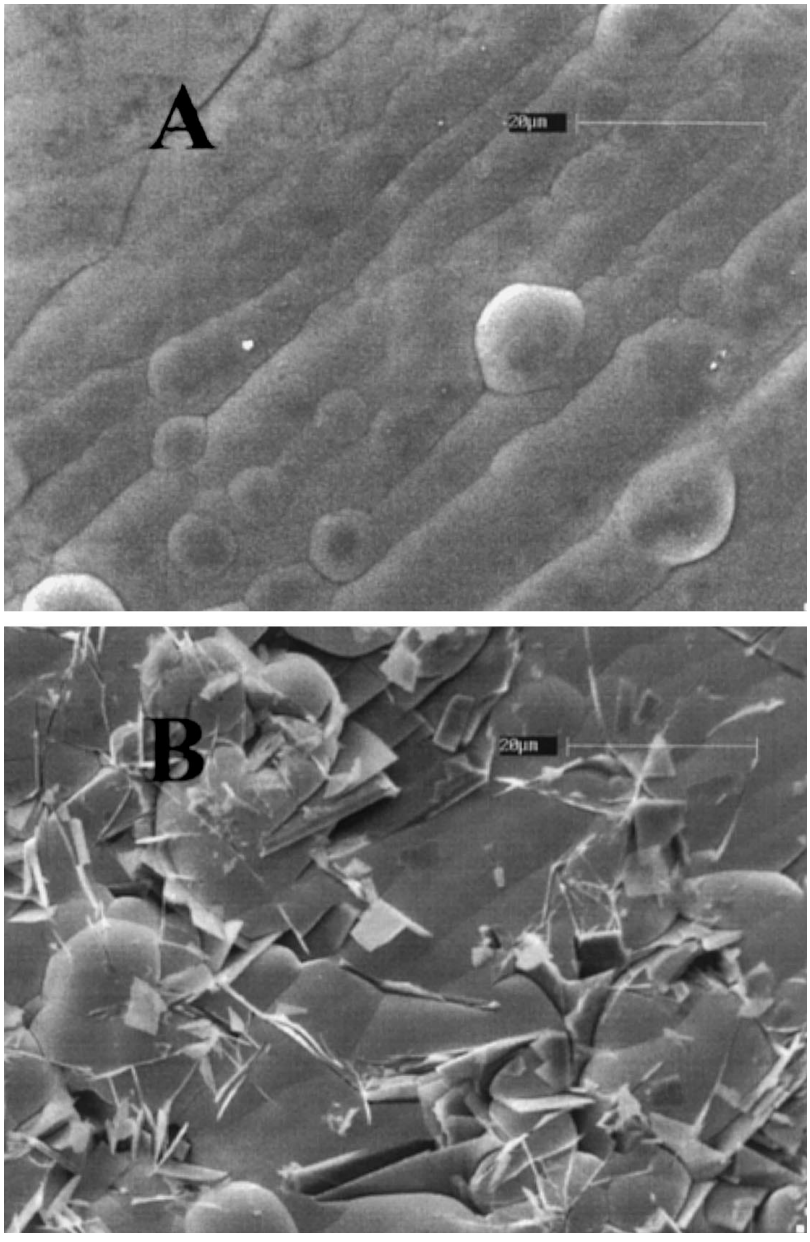

Fig. 7A, B Micrographs of the surface of Fe-W amorphous layers obtained under optimum conditions (**B**) and in a bath at pH 5.5 (**A**)

Table 1 Comparison of the lattice parameters of Fe, Co, and Ni and their amorphous alloys with tungsten

	Fe(110)	Fe-W	Co(111)	Co-W	Ni(111)	Ni-W	W(110)
2Θ	52.47	50.1	52.83	51.6	52.20	51.1	47.15
d (Å)	2.027	2.111	2.047	2.057	2.034	2.077	2.238

Table 2 Influence of tungsten content on mean inter-atom distance in Co-W, Ni-W, and Fe-W amorphous alloys

x : *y*	Fe_x-W_y		*x* : *y*	Co_x-W_y		*x* : *y*	Ni_x-W_y	
	2Θ max	*d* (Å)		2Θ max	*d* (Å)		2Θ max	*d* (Å)
16 : 84	52.05	2.040	15 : 85	52.05	2.047	14 : 86	51.92	2.046
22 : 78	51.80	2.049	19 : 81	51.85	2.051	20 : 80	51.41	2.063
28 : 72	50.60	2.094	26 : 74	51.55	2.061	25 : 75	51.07	2.077
38 : 62	50.16	2.123	34 : 66	51.10	2.075	31 : 69	51.09	2.076

Table 3 Comparison of the composition of tungsten amorphous alloys and intermetallic compounds formed by tungsten with nickel, cobalt, and iron

W and Ni		W and Co		W and Fe	
Crystalline	Amorphous	Crystalline	Amorphous	Crystalline	Amorphous
Ni_4W NiW NiW_2	$Ni_{77}W_{23}$	Co_3W Co_7W_6	$Co_{72}W_{27}$	Fe_2W Fe_3W_2	$Fe_{62}W_{38}$

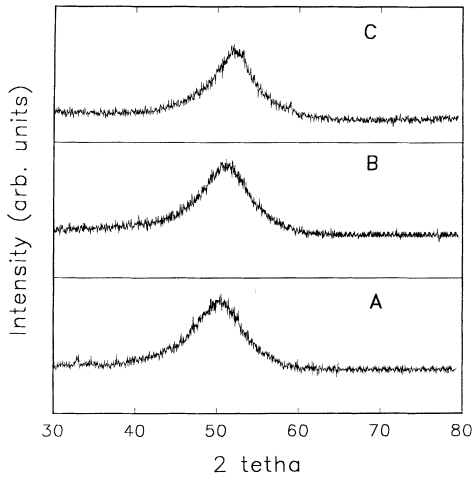

Fig. 8A–C X-ray diffractograms obtained for Fe-W (**A**), Co-W (**B**), and Ni-W (**C**). Alloys were electrodeposited from citrate baths on a copper substrate

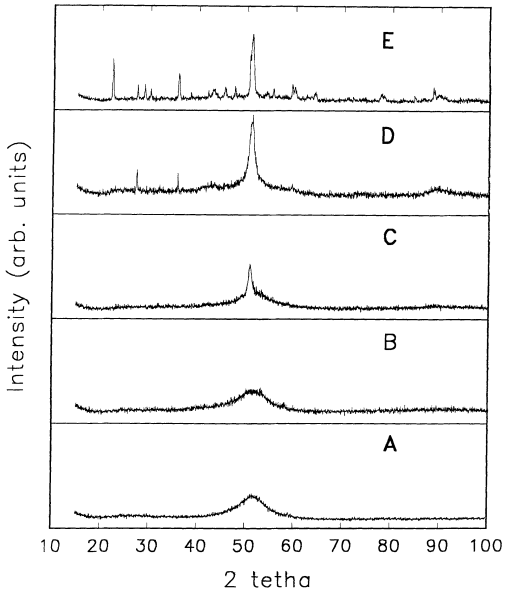

Fig. 9A–E X-ray diffractograms obtained for Ni-W alloy: as deposited (**A**) and heated under vacuum for 2 h at 200 (**B**), 400 (**C**), 500 (D) and 650 °C (**E**)

Also, the fact that, in the alloys deposited by Rauscher et al., tungsten oxides appeared only in one of three analyzed samples may suggest that a WO_x phase can be

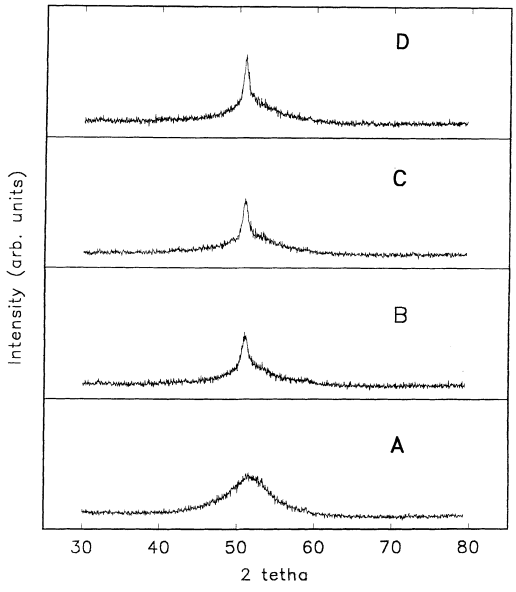

Fig. 10A–D X-ray diffractograms obtained for Ni-W alloy as deposited (**A**) and heated at 400 °C for 1 (**B**), 2 (**C**) and 4 h (**D**) under vacuum

deposited only under specific conditions, different from those existing in the plating process described in this work. The conditions leading to the presence of oxides in the Fe-W alloys were identified in this paper as deposition in a bath of pH 5.5 or less.

The results of the X-ray diffraction analysis of electrodeposited alloys suggest that the internal organization of electrodeposited materials is similar to a solid solution of tungsten in an iron-group metal. The very weak internal organization of the tungsten alloys is probably that of a highly deformed iron-group metal. The constitution of an amorphous-like structure can be promoted by parallel incorporation of tungsten into the iron-group metal lattice and intensive hydrogen evolution. It is possible that the codeposition of hydrogen into the metal layer promotes the formation of a glass structure of the metal.

The glass structure of the alloys increases its internal order during heat treatment at approximately 400 °C. At this temperature the crystallization process is limited to the homogeneous alloy structure of probably the solid solution type. An increase in the heating temperature up to 650 °C leads to consecutive crystallization of the alloy. It is seen that at 650 °C the formation of a new phase

occurs. It resembles the crystallization case for glasses first crystallized to a metastable phase being homogeneous apart from local defects. Upon further heat treatment the homogeneous phase disintegrates into a variety of crystalline forms. This model of the crystallization process is typical for the solid-solution type metallic glasses [17–19].

Acknowledegments The author thanks Ulf Jensen from the Jan Otto Carlson group in Uppsala University for making possible the ESCA measurements and for helpful assistance in interpretation of the spectra obtained. This work was supported by grant no. BW-1387/9/97 from the University of Warsaw.

References

1. Klement W Jr, Willens RH, Duwez P (1960) Nature 187: 869
2. Bagley BG, Turnbull D (1968) J Appl Phys 39: 5681
3. Watanabe T (1987) J Met Finish Soc Jpn 38: 2104
4. Brunch A (1989) J Appl Phys 50: 7603
5. Ennas G, Magini M, Padella F, Susani P, Boffitto G (1989) J Mater Sci 24: 3053
6. Akahama Y, Mori Y, Kobayashi M, Kawamura H, Kimura K (1989) J Phys Soc Jpn 58: 2231
7. Archer MO, Corke CC, Harji BH (1987) Electrochim Acta 32: 13
8. Shinada Y, Manabu T (1993) Jpn Pat 93 222 588
9. Nakazawa B (1989) Amorphous Plating 3: 13
10. Donten M, Stojek Z, Osteryoung JG (1990) J Electrochem Soc 140: 3417
11. Bard A (ed) (1972) Encyclopedia of electrochemistry of the elements, vol 2. Dekker, New York
12. Croopnik GA, Scruggs DM (1985) US Pat 4 529 668
13. Donten M, Stojek Z (1994) Pol J Chem 68: 1193
14. Donten M, Osteryoung JG (1990) J Appl Electrochem 20: 671
15. Wikieł K, Osteryoung JG (1992) J Appl Electrochem 22: 506
16. Rauscher G, Rogoll V, Baougaertner ME, Raub ChJ (1993) Trans Inst Met Finish 71: 95
17. Heusler KE, Huerta D (1989) J Electrochem Soc 136: 65
18. National Research Council (1985) Report on artificially structured materials. National Academy Press, Washington
19. Watanabe T (1993) In: Sakurai Y, Hamakawa Y, Shirae K, Suzuki K (eds) Current topics in amorphous materials: physics and technology. Amsterdam p 137
20. Nagender Naidu SV, Rama Rao P (eds) (1991) Phase diagrams of binary tungsten alloys. Indian Institute of Metals, Calcutta, pp 60–69, 89–102, 170–178
21. Boom R, de Boer FR, Nilssen AK, Miedema AR (1983) Physica B 115: 285
22. Nilssen AK, Miedema AR, de Boer FR, Boom R (1988) Physica B 152: 303
23. Nilssen AK, Miedema AR, de Boer FR, Boom R (1988) Physica B 152: 401